Vibrational Spectra of Individual Millimeter-Size Membrane Patches Using Miniature Infrared Waveguides

Susan E. Plunkett, Roy E. Jonas, and Mark S. Braiman
University of Virginia Health Sciences Center, Department of Biochemistry, Charlottesville, Virginia 22908 USA

ABSTRACT We have used miniature planar IR waveguides, consisting of Ge strips 30–50 μm thick and 2 mm wide, as evanescent-wave sensors to detect the mid-(IR) evanescent-wave absorbance spectra of small areas of biomolecular monolayers and multilayers. Examples include picomolar quantities of an integral transmembrane protein (bacteriorhodopsin) and lipid (dimyristoyl phosphatidylcholine). IR bands due to the protein and lipid components of the plasma membrane of individual 1.5-mm-diameter devitellinized *Xenopus laevis* oocytes, submerged in buffer and sticking to the waveguide surface, were also detected. A significant improvement in sensitivity was observed, as compared to previous sizes and geometries of evanescent-wave sensors (e.g., commercially available internal reflection elements or tapered optical fibers). These measurements suggest the feasibility of using such miniature supported planar IR waveguides to observe structural changes in transmembrane proteins functioning in vivo in single cells.

INTRODUCTION

Fourier transform infrared (FTIR) spectroscopy is a well-established technique for studying biological membranes, and in particular membrane proteins, for which there are few x-ray crystal structures (Braiman and Rothschild, 1988; Fringeli and Gunthard, 1980). To study biological membranes in their native environment with IR, a surface sensitive technique is needed. Transmission experiments are limited by strong water absorption to very short pathlengths (~10 μm). Hence, thin-film samples that need to be in contact with bulk water are most effectively measured by attenuated total reflection (ATR) spectroscopy, also known as evanescent-wave spectroscopy (EWS) (Harrick, 1979). With this technique, IR light passing through a material of high refractive index undergoes total internal reflection at the interface(s) with media of lower refractive index. At each internal reflection, an evanescent field propagating in a direction tangential to the surface penetrates a fraction of the wavelength of the light into the outer medium, where it can be absorbed by molecules within ~1 μm of the surface.

There have been many studies of biological samples coating the large sampling surfaces of commercially available ATR optical elements (e.g., 50 × 1 × 20 mm) designed for use with standard FTIR spectrometers. Examples of biomembrane samples include peptides incorporated into thick multibilayers of lipid (Fringeli, 1980), lipid monolayers exposed to air (Briggs et al., 1986), and individual supported bilayers exposed to bulk water (Frey and Tamm, 1991; Smith et al., 1994). These studies have generally required a minimum sample size on the order of 1 μg. When only smaller samples are available, however, smaller ATR elements are called for.

Mid-IR transmitting optical fibers have provided a useful demonstration of the increased sensitivity of micro-ATR optical elements for small sample sizes (Simhony et al., 1988; Compton et al., 1988). In an early application, Braiman and Wilson (1989) used IR optical fibers (in this case 500 μm in diameter), along with a standard FTIR spectrometer, to obtain ATR spectra of biomembrane samples. Subsequently, Braiman and Jonas utilized a chalcogenide fiber optic ATR element with single-membrane-thick samples (Jonas and Braiman, 1993a), detecting amide I and amide II absorption signals from an ion-channel-forming peptide (alamethicin) that had been inserted into a supported lipid bilayer coated onto a 15-cm length of fiber (Braiman and Jonas, 1992).

A cylindrical fiber geometry is not conducive to maximum contact area, which affords optimized sensitivity, for certain biological samples, such as the membrane of a large cell or a film applied by traditional Langmuir-Blodgett techniques. Other disadvantages of a cylindrical (fiber) geometry include difficulties in fabricating an uncoated self-supporting fiber of an optimal thickness (50 μm or less); difficulties in obtaining the large bevel or launch angle needed to optimize the evanescent field penetration depth, the interfacial evanescent field intensity, and the number of internal reflections; and an inability to obtain spectra with light of different polarizations (to measure linear dichroism and thus obtain information about the orientation of particular bonds with respect to the membrane normal).

Planar waveguides present an alternative to optical fibers that may alleviate some of these problems. We have recently designed and fabricated supported planar Ge waveguides (50 μm × 2 mm × 12 mm) and have shown that an IR microscope can be used to couple adequate amounts of light into and out of the waveguide for obtaining evanescent-wave absorption spectra (Plunkett et al., 1997). As shown below, these waveguides have now permitted the

Received for publication 10 April 1997 and in final form 8 July 1997.

Address reprint requests to Dr. Mark S. Braiman, Department of Biochemistry, no. 440, University of Virginia Health Sciences Center, Charlottesville, VA 22908-0001. Tel.: 804-924-5062; Fax: 804-924-5069; E-mail: msb7e@virginia.edu.

0006-3495/97/10/2235/06 $2.00

measurement of a multiple-internal-reflection infrared (MIRIR) spectrum of the surface of individual 1.5-mm-diameter frog (*Xenopus laevis*) oocytes. We compare these results to the MIRIR spectrum of the same cell type, taken through a chalcogenide fiber coupled to a standard FTIR spectrometer. In addition, several simpler model systems, involving monolayers of bacteriorhodopsin (bR), a protein, and dimyristoylphosphatidylcholine (DMPC), a lipid, were measured to calibrate the waveguide's sensitivity.

MATERIALS AND METHODS

Infrared evanescent-wave sensor fabrication and optical alignment

Chalcogenide optical fibers

The design of tapered chalcogenide fiber optic sensors has been described previously (Jonas and Braiman, 1993a,b; Braiman and Jonas, 1992). Briefly, 0.5-mm-diameter AsSeTe chalcogenide IR fiber was obtained from Amorphous Materials (Garland, TX). A short length of this fiber was tapered to a 0.2-mm diameter over a ~1-cm length, by manually pulling on its ends while the center was softened with a heat gun. This tapered fiber was then cleaved ~6 mm away from the taper on both sides and was carefully inserted into a 0.5-mm-diameter hole predrilled ~3 mm from the top of a custom-fabricated poly(tetrafluoroethylene) (PTFE) trough. A shallow cylindrical section of this 10-mm-wide trough had also been machined away from its top, at right angles to the 0.5-mm fiber hole, to expose just the central portion of the fiber hole.

Thus, after insertion of the fiber and filling of the trough with buffer solution, the central taper of the fiber was exposed to the aqueous buffer, and the thicker outer portions were held snugly in two colinear holes in the PTFE, preventing leakage of the buffer solution through those holes. Plastic tape around the perimeter of the trough and extending up from its top edges helped to contain the buffer solution. The fiber ends were cleaved flush with the outer surfaces of the PTFE trough.

The trough and fiber were mounted inside the microbeam compartment of a Nicolet 60SXR, with the fiber colinear with the optical axis. The trough was positioned so that the *f*/1 condensing mirror of the microbeam compartment focused the IR light onto one fiber end. The *f*/1 collecting mirror was then carefully adjusted to collect light from the other end of the fiber. Additional microbeam compartment optical elements were used to focus light onto one end of the fiber, and from the other end of the fiber onto a narrowband (0.25 mm)^2 Hg-Cd-Te (MCT-A) detector from Belov Technology Co. (New Brunswick, NJ).

Supported planar Ge waveguides

Infrared waveguides were fabricated from commercially available prisms of Ge and ZnS, as described previously (Plunkett et al., 1997). A 12 × 2 × 2-mm Ge orthorhomb, coated on one side with a 2-μm-thick cladding layer of ZnS and then cemented to a larger ZnS substrate, was ground and polished by hand to a final thickness of 30–50 μm. Beveled edges of 45° were also ground and polished on the waveguide (as well as the top of the substrate), by using PTFE guides cut to the desired angle. Large refractive index differences enabled the resulting thin film of Ge (n = 4.0), sandwiched between ZnS (n = 2.2) and air (n = 1.0) or water (n = 1.34), to act as a waveguide for IR light.

Broadband infrared light was coupled into and out of the ends of the waveguide and was measured using an IR-Plan infrared microscope (Spectra-Tech, Stamford, CT) interfaced to an FTIR spectrometer. This IR microscope was selected because it is one of the only models available that permits the separate focusing of the objective and condenser mirrors on the input and output ends of the waveguide, some 12 mm apart. The waveguide was thus mounted with the light traveling along the vertical optical axis of the microscope.

A special PTFE trough was designed to girdle the waveguide-coated substrate, allowing frog oocyte samples to be kept submerged in isotonic solution and simultaneously in contact with the vertically mounted waveguide. Light passing through the waveguide was collected from its bottom end by the microscope's condensor element and was focused onto a photoconductive HgCdTe detector with a (0.1 mm)^2 active area (Graseby Infrared, model FTIR-M16-0.10). Data processing was done with GRAMS 386 software (Galactic Industries, Salem, NH). All spectra shown below were obtained by using 10,000 coadded scans, with 8 cm^{-1} spectral resolution and a spectral sampling range of 7900–0 cm^{-1}.

Sample preparation

Bacteriorhodopsin films

All bacteriorhodopsin (bR) used was in the form of purple membranes prepared from *Halobacterium salinarium* strain S9 (Oesterhelt and Stoeckenius, 1974). The bR stock solution was washed three times with deionized water (pelleted at 5000 × g and resuspended) to remove the 4 M salt present in the storage buffer. An aqueous volume of 0.5 μl was found to form a droplet of 3-mm diameter when placed on the Ge waveguide and substrate. For IR measurements, one or more 0.5-μl aliquots of a 2.1 μM suspension were placed on the Ge waveguide, then allowed to evaporate under a dry-air atmosphere for ~20 min before IR measurements.

Pure lipid films

DMPC was purchased from Avanti Polar Lipids (Alabaster, AL) and used without further purification. For IR measurements, 0.5-μl aliquots of the stock lipid solution (0.10 mg/ml or 132 μM in $CHCl_3$) were evaporated onto the surface of the waveguide.

Single frog oocytes

Freshly harvested oocytes from *Xenopus laevis* were graciously provided by Edward Johns and Randall Moorman, and were processed by published procedures (Mounsey et al., 1995). The eggs were defolliculated by exposure to collagenase with gentle mechanical disruption, and were stored for up to 2 days in Barth's solution at 4°C. The vitelline membrane was partially removed immediately before IR measurements, by transferring the oocyte to hypertonic solution for 5 min, then transferring back to isotonic solution and carefully dissecting a portion of the vitelline membrane with fine surgical tweezers. Only eggs that remained unbroken at this point were used for spectrometry.

A plastic pipette was used to transfer an egg, in isotonic buffer, to the PTFE trough machined to fit around the fiber or planar waveguide (see descriptions above). A background spectrum was collected with the egg sitting several millimeters away from the waveguide or fiber; then the egg was gently propelled, using brief expulsions of buffer from the pipette, until its exposed plasma membrane contacted the waveguide. Once this contact was made, the egg was fixed in position, because its exposed bilayer membrane adhered quite well to the rather hydrophilic surface of the chalcogenide fiber or Ge waveguide. However, breakage of an egg during any part of this procedure, which occurred occasionally, resulted in discarding it (and the background data), careful washing of the waveguide and trough to remove all traces of biological material, and realignment for new background and sample measurements with a different, freshly devitellinized egg in the trough.

RESULTS AND DISCUSSION

We first obtained spectra of two well-characterized biological samples to determine the sensitivity and accuracy of the

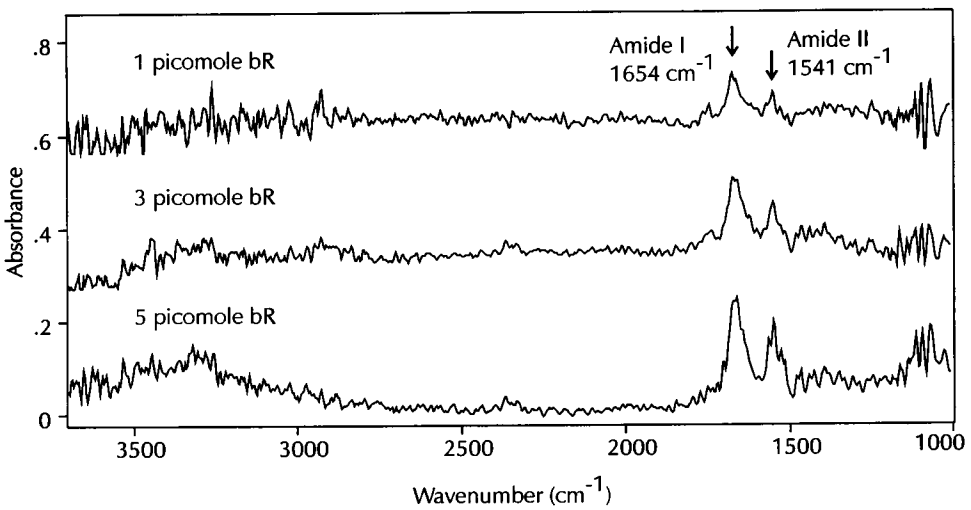

FIGURE 1 The FTIR evanescent-wave absorption spectra of 1, 3, and 5 pmol of bR (25, 75, and 125 ng of protein, respectively), measured using a 50-μm Ge waveguide with 45° bevel angles as an internal reflection element. The amide I and amide II absorption bands of the protein at 1654 and 1541 cm^{-1} decrease linearly with decreasing sample size; the limit of detection is clearly <25 ng protein.

planar waveguide, and to provide comparisons to the protein and lipid bands in the oocyte spectrum. Fig. 1 presents evanescent-wave IR spectra of dried bR (purple membrane) films 2 × 2 mm in area. From top to bottom, these three films correspond in thickness to a monolayer (1 pmol of bR spread over a 3-mm-diameter area), and to 3 and 5 times this amount. The two most prominent bands in each spectrum, at 1654 and 1541 cm^{-1}, are the well-known amide I and amide II vibrations. These bands are definitively from bR, because successive applications of more sample (to produce multiple 2 mm × 2 mm patches along the 12-mm length of the planar guide) caused these bands to increase in intensity. A transmission spectrum of a thick film of the same bR solution dried onto a CaF_2 window had bands at the same wavenumber positions with the same relative intensities (data not shown).

As the sample size increased (from 1 to 3 to 5 pmol of bR), the absorbance values for both the amide I and amide II bands increased proportionally. As noted previously (Jonas and Braiman, 1993a), multimode evanescent-wave spectra often exhibit significant nonlinear behavior at absorbance values above ~0.1, which complicates quantitative analyses. However, in this case the use of a high-index waveguide with parallel surfaces and fixed bevel angles on the ends apparently limits the number of modes propagating, resulting in rather good linearity.

Fig. 2 is the evanescent-wave IR spectrum of a dry film of DMPC containing 66 pmol of lipid (0.5 μl of 132 μM stock solution) spread over a ~13-mm^2 area of the waveguide (2 mm wide × 6.5 mm long). This is approximately the amount of lipid that would be present in a single lipid bilayer covering the same area (which would have a lipid surface concentration of 0.5 nmol/cm^2, corresponding to the known area of 60–70 $Å^2$ per lipid headgroup in a bilayer). The strongest bands are the C—H stretch vibrations around 2900 cm^{-1} and the C=O ester stretch at 1741 cm^{-1}. Their frequencies, bandshapes, and relative intensities correspond well to the bands observed in the transmission spectrum of the same lipid solution dried onto a CaF_2 window (data not shown).

Fig. 3 *B* presents evanescent-wave IR spectra of a single oocyte, 1.5 mm in diameter, in contact with a 50-μm-thick,

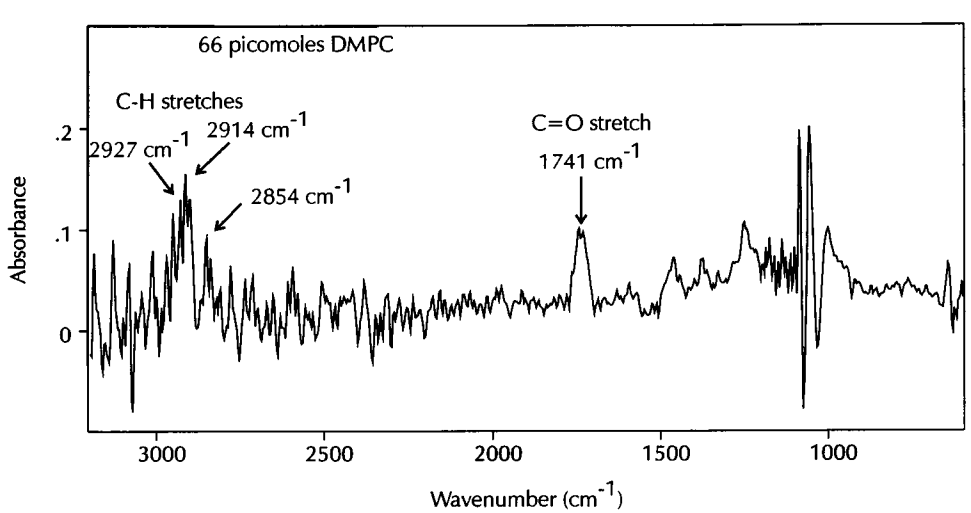

FIGURE 2 The FTIR evanescent-wave absorption spectrum of the equivalent of a single bilayer of DMPC covering a 13-mm^2 portion of the surface of the 50 μm × 2 mm × 13 mm Ge waveguide with 45° bevel angles. The lipid asymmetrical (2900 cm^{-1}) and symmetrical (2854 cm^{-1}) C—H stretch vibrations and the lipid C=O stretch (1741 cm^{-1}) are easily detected.

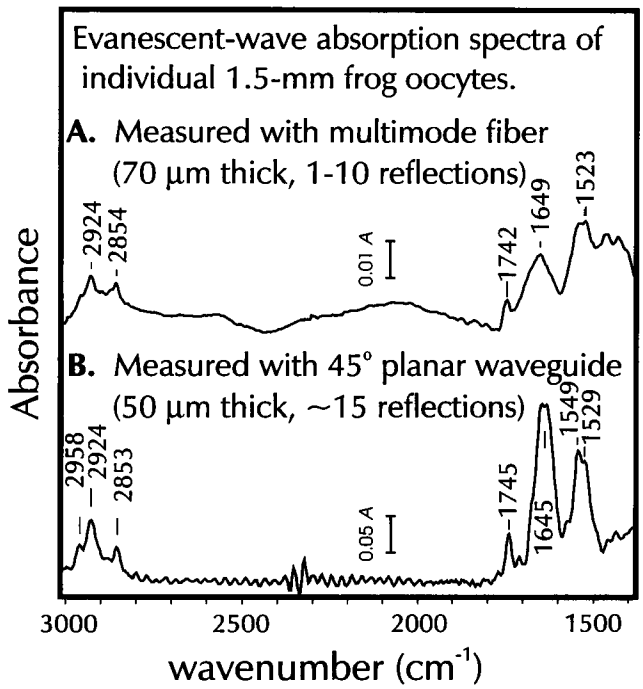

FIGURE 3 (*A*) FTIR evanescent-wave absorption spectrum of a 1.5-mm-diameter oocyte on the 70-μm-thick, 3-mm-wide tapered and flattened sensing region of a 10-mm length of 500-μm-diameter chalcogenide (AsSeTe) fiber. Oocyte protein and lipid bands correspond to the bands observed in the absorbance spectra of similarly-sized model protein (bR) and lipid (DMPC) samples. (*B*) FTIR evanescent-wave absorption spectrum of a similarly prepared oocyte, measured using an 80-μm-thick, 3-mm-wide supported planar Ge waveguide with 45° bevel angles at both ends. The lipid and protein bands (*marked bands*) exhibit slightly higher absorbance than for an oocyte in contact with a tapered fiber of similar thickness and threefold narrower width (*A*). This is principally due to the exclusive propagation through the beveled waveguide of higher order modes (light propagating closer to the normal to the oocyte-waveguide interface), which led to a greater penetration depth and evanescent-wave surface intensity than was obtained in the tapered multimode fiber.

2-mm-wide Ge waveguide. It is compared to the spectrum of a similar oocyte in contact with a chalcogenide fiber sensor tapered to a 70-μm thickness (Fig. 3 *A*). Key biomolecular vibrational features are quite similar in the two spectra. The asymmetrical and symmetrical C—H stretch vibrations of lipid side chains are observed at 2924 ± 1 and 2854 ± 2 cm^{-1}, respectively, and the lipid ester vibration is centered at 1744 ± 2 cm^{-1}. These frequencies are very similar to those of the pure lipid film in Fig. 2.

On the other hand, the observed bandshapes of the amide I and amide II vibrational bands of the oocyte spectra depend somewhat on whether the fiber or planar waveguide was used for the measurement. Both amide I and amide II bands are also shifted somewhat relative to the corresponding bands observed for bacteriorhodopsin (see Fig. 1 above). These shifts are all probably an authentic reflection of differences in secondary structure of the particular sets of proteins being sampled. Bacteriorhodopsin consists predominantly of transmembrane α-helices, which are generally observed to have amide I vibrational band frequencies near 1655 cm^{-1} (see, for example, Smith et al., 1994). In contrast, with both the fiber and the planar waveguide measurements of the intact oocyte, it is expected that a mix of different membrane proteins is being measured, including some with nonhelical portions. Furthermore, the evanescent wave penetration depth (~1 μm) is substantially greater than the membrane thickness. Therefore, evanescent-wave measurements of the intact oocyte are detecting IR absorption not only from proteins within the plasma membrane, but also from proteins within a thin (~1 μm) layer of cytoplasm immediately inside the membrane.

It is noteworthy that the detected absorbance values are substantially greater for the planar Ge waveguide than for the tapered chalcogenide fiber, despite the fact that similar lengths of the fiber and waveguide were in contact with the oocyte. Part of the difference is due to the fact that the waveguide was somewhat thinner (50 μm versus 70 μm tapered fiber), and part is due to the coupling of the IR light with much higher (farther off-axis) propagation angles by the 45°-beveled waveguide ends than by the unbeveled fiber ends. Both of these changes are expected to increase the number of reflections per unit length, whereas the increase in propagation angle is also expected to increase the evanescent field's strength as well as its depth of penetration into the sample. These increases in evanescent field strength and penetration depth are expected to be only partially counteracted by decreases due to the larger refractive index of Ge (n = 4.0), as compared to the AsSeTe fiber (n = 2.8).

The greater average penetration depth with the beveled planar waveguide versus the tapered fiber may also account for the fact that the relative intensities (and band shapes) of the measured amide absorptions vary somewhat for the oocyte samples using the two different types of evanescent-wave sensors. For instance, the 1625 cm^{-1} component of the amide I band, which is characteristic of β-sheet (Susi and Byler, 1986) and coiled-coil (Heimburg et al., 1996) structures, appears to be relatively greater in the spectrum measured with the waveguide (Fig. 3 *B*) than in the spectrum measured with the fiber (Fig. 3 *A*). This could be consistent with the greater penetration depth of the Ge waveguide resulting in a deeper sampling of the cytoplasm, including proteins with such secondary structures, whereas the membrane proteins that are more likely to be composed of simple α-helices (which is expected to have an amide I mode near 1650 cm^{-1}, as in the case of bacteriorhodopsin) are more selectively sensed by the lower propagation angles within the tapered fiber.

Despite the apparently greater sampling of cytoplasm by the beveled planar waveguide than by the tapered fiber, the planar waveguide may represent a superior approach for detecting the IR absorption of the membrane components (both lipid and protein) of a large single cell such as an oocyte. It should be possible to fabricate bitapered planar waveguides with unbeveled ends, while maintaining the absorption strength from the membrane proteins by making the waveguides somewhat thinner than 50 μm, as proposed recently (Braiman and Plunkett, 1997). Such quasiplanar

tapered waveguides should give a range of penetration depths that generally resemble those of the bitapered fiber, and should thus reduce the relative contribution of cytoplasmic proteins to the spectrum, relative to the measurement in Fig. 3 *B*, while still maintaining sensitivity to membrane components. Our group has recently fabricated planar (untapered) Ge waveguides as thin as 30 μm with adequate IR transmission for evanescent-wave measurements (J. J. Stone and M. S. Braiman, unpublished data). On the other hand, we have found it difficult to mount an oocyte against a naked chalcogenide fiber much thinner than 50 μm, or to cleave a fiber end at an angle much greater than ~15°. Thus, using a fiber, we are unlikely to be able to improve much over the measurements shown in Fig. 3 *A*.

Furthermore, it is unlikely that a polarization-preserving cylindrical fiber can be easily fabricated, whereas a planar waveguide with a large width/thickness ratio should preserve polarization and therefore be useful for dichroism measurements such as have traditionally been performed with large internal reflection elements in ATR-IR spectroscopy. Thin planar waveguides thus promise more sensitivity and versatility than chalcogenide fibers for single-cell measurements.

Fig. 4 is a plot of the DMPC lipid ester C=O stretch absorbance intensity for one-bilayer-thick samples of biomembrane, versus the number of internal reflections using various biomembrane sources, evanescent-wave sensor types, and sample-sensor interaction lengths. It is evident from this plot that when a single-bilayer-membrane film is being sensed, the measured absorbance due to the lipid ester C=O vibration is linearly correlated with the number of reflections. This is true regardless of whether the variation in number of reflections is obtained by varying the length or the thickness of the sensor. However, the lipid ester absorption strength from the oocyte falls considerably above that predicted by the plot for pure lipid bilayers. This suggests that within the ~1-μm penetration depth of the evanescent wave, there are many more lipid molecules than just those found within the membrane bilayer itself. Nevertheless, the size of the ester C=O band obtained with the supported planar waveguide was reproducible with different egg cells, and the oocytes were quite clearly intact during the measurement, ruling out the possibility that the oocyte contents leaked out and spread over a longer portion of the waveguide than indicated. It is possible that a high concentration of lecithin molecules within the cytoplasm (or yolk) of the oocyte are being detected by the ATR measurement.

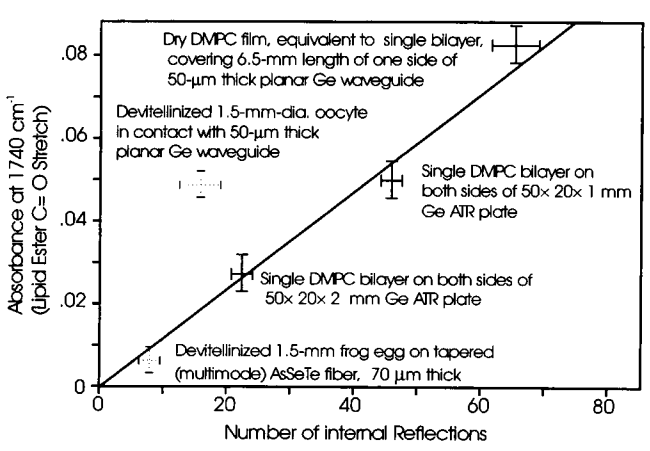

FIGURE 4 Correlation of the lipid ester carbonyl stretch absorbance intensity (maximum intensity at ~1740 cm^{-1} of the best-fit Gaussian band shape) with the number of internal reflections. For the multimode measurements (e.g., using tapered optical fiber), a broad range of reflection numbers apply. Nevertheless, a roughly linear relationship is observed, even for planar sensors as thin as 50 μm. The types of sample and evanescent-wave sensor used for each plotted measurement are indicated.

It seems clear from the data obtained on pure lipid films that the measured absorbance of the lipid in a single-bilayer film covering a tiny surface area can attain values as high as more traditional measurements of large supported bilayer films using macroscopic ATR optical elements (Frey and Tamm, 1991; Smith et al., 1994), as long as the waveguide used for the measurement has a comparably large number of reflections (e.g., 40–50) along its surface in contact with the patch. For an interaction length of ~1 mm, this will require a waveguide of thickness on the order of 10 μm. This is several times thinner than the waveguides described in this communication. With waveguides this thin, we might expect to detect IR absorption spectra from subpicomolar samples.

Other analytical techniques (e.g., mass spectrometry, fluorescence spectroscopy) are known to be capable of sensing even less than a picomole of biomolecules in an individual intact cell. For example, in combination with confocal microscopy, fluorescence measurements have already been used to detect voltage-gated conformational changes of femtomole quantities of *Shaker* K^+ channels expressed in individual *Xenopus* oocytes (Mannuzzu et al., 1996). The high sensitivity of such fluorescence measurements stems in part from their sensing the emission of visible photons, i.e., a zero-background method in which nearly all of the detected energy is signal. In FTIR absorption measurements, on the other hand, a small change in transmitted intensity must be detected in the presence of a relatively large background IR intensity that contributes shot noise.

On the other hand, visible fluorescence involves electronic transitions, the absorption bands of which characteristically are very broad. Fluorescence bands therefore are relatively easy to detect, but do not provide as detailed structural information as the narrow vibrational bands in IR spectroscopy. Furthermore, sensitive visible fluorescence measurements such as those recently published on voltage-gated proteins in single oocytes (Mannuzzu et al., 1996) have depended on site-directed labeling of the protein with an extrinsic fluorophore, whereas IR spectroscopy provides useful information about a wide variety of intrinsic chemical groups that are themselves active in membrane protein mechanisms, e.g., side chains of charged amino acids as well as peptide backbone groups. Therefore, evanescent-wave IR spectroscopy of membrane proteins in single cells

might provide useful structural information about protein conformation that is not available from the other methods.

CONCLUSION

We have demonstrated the usefulness of miniature planar Ge waveguides for making IR evanescent-wave absorption measurements of very small biological samples, including the membranes of individual intact *Xenopus* oocytes. Our ultimate aim—detecting conformational changes of voltage-gated ion channels and other transmembrane proteins expressed in frog oocytes—will depend on further development of evanescent-wave sensors, because femtomolar sensitivity will be needed. To achieve this goal, however, it should only be necessary to increase by 2–3 orders of magnitude the evanescent field intensity at the surface of a planar waveguide (relative to the total energy flux through the guide). It should be possible to accomplish this by decreasing the waveguide thickness and width at the sensing area, by a factor of ~30-fold each. While such tiny waveguides can in theory transmit sufficient total broadband light energy to make the measurements with the required signal-to-noise ratio, obtaining adequate energy throughput will require very efficient light coupling methods, probably involving specially fabricated waveguides with gradually tapered thickness and width.

We are grateful to Ed Johns and Randall Moorman for providing frog oocytes, and to David Hunter Matthews for his assistance in preparing the oocytes for spectroscopy. This work was supported by National Science Foundation grant MCB-9406681 to MSB. The IR microscope and spectrometer were obtained through a shared instrumentation grant (S10 RR08959) from the National Institutes of Health.

REFERENCES

Braiman, M. S., and R. E. Jonas. 1992. Evanescent-wave IR spectroscopy of single-bilayer membranes coated on chalcogenide fibers: sensitivity improvements using a diamond rod coupler between fiber and source. *Proc. SPIE.* 1796:402–411.

Braiman, M. S., and S. E. Plunkett. 1997. Design for supported planar waveguides for obtaining mid-IR evanescent-wave absorption spectra from biomembranes of individual cells. *Appl. Spectrosc.* 51:592–597.

Braiman, M. S., and K. J. Rothschild. 1988. Fourier transform infrared techniques for probing membrane protein structure. *Annu. Rev. Biophys. Biophys. Chem.* 541–570.

Braiman, M. S., and K. J. Wilson. 1989. New FTIR techniques for studying biological membranes. *Proc. SPIE.* 1145:397–399.

Briggs, M. S., D. G. Cornell, R. A. Dluhy, and L. M. Gierasch. 1986. Conformations of signal peptides induced by lipids suggest initial steps in protein export. *Science.* 233:206–208.

Compton, D. A. C., S. L. Hill, N. A. Wright, M. A. Druy, J. Piche, W. A. Stevenson, and D. W. Vidrine. 1988. In situ FT-IR analysis of a composite curing reaction using a mid-infrared transmitting optical fiber. *Appl. Spectrosc.* 42:972–979.

Frey, S., and L. K. Tamm. 1991. Orientation of melittin in phospholipid bilayers: a polarized attenuated total reflection infrared study. *Biophys. J.* 60:922–930.

Fringeli, U. P. 1980. Distribution and diffusion of alamethicin in a lecithin/water model membrane system. *J. Membr. Biol.* 54:203–212.

Fringeli, U. P., and H. H. Gunthard. 1981. Infrared membrane spectroscopy. *Mol. Biol. Biochem. Biophys.* 31:270–332.

Harrick, N. J. 1979. Internal Reflection Spectroscopy. Harrick, Ossining, NY.

Heimburg, T., J. Schuenemann, K. Weber, and N. Geisler. 1996. Specific recognition of coiled coils by infrared spectroscopy: analysis of the three structural domains of type III intermediate filament proteins. *Biochemistry.* 35:1375–1382.

Jonas, R. E., and M. S. Braiman. 1993a. Efficient source-to-fiber coupling method using a diamond rod: theory and application to multimode evanescent-wave IR absorption spectroscopy. *Appl. Spectrosc.* 47: 1751–1759.

Jonas, R. E., and M. S. Braiman. 1993b. Compact source-to-fiber diamond optical coupler enhances absorbances from optical fiber evanescent-wave IR spectroscopy using a simple design. *Proc. SPIE.* 1886:9–14.

Mannuzzu, L. M., M. M. Moronne, and E. Y. Isacoff. 1996. Direct physical measure of conformational rearrangement underlying potassium channel gating. *Science.* 271:213–216.

Mounsey, J. P., P. Xu, J. E. John, L. T. Horne, J. Gilbert, A. D. Roses, and J. R. Moorman. 1995. Modulation of skeletal muscle sodium channels by human myotonin protein kinase. *J. Clin. Invest.* 95:2379–2384.

Oesterhelt, D., and W. Stoeckenius. 1974. Isolation of the cell membrane of *Halobacterium halobium* and its fractionation into red and purple membranes. *Methods Enzymol.* 31:667–678.

Plunkett, S. E., S. Propst, and M. S. Braiman. 1997. Supported planar germanium waveguides for infrared evanescent-wave sensing. *Appl. Optics.* 36:4055–4061.

Simhony, S., A. Katzir, I. Schnitzer, and E. M. Kosower. 1988. Evanescent wave infrared spectroscopy of liquids using silver halide optical fibers. *J. Appl. Phys.* 64:3732–3734.

Smith, S. O., R. Jonas, M. Braiman, and B. J. Bormann. 1994. Structure and orientation of the transmembrane domain of glycophorin A in lipid bilayers. *Biochemistry.* 33:6334–6341.

Susi, H., and D. M. Byler. 1986. Resolution-enhanced Fourier transform infrared spectroscopy of enzymes. *Methods Enzymol.* 130:290–311.